13th International Conference on Aluminum Alloys (ICAA13)
Edited by: Hasso Weiland, Anthony D. Rollett, William A. Cassada
TMS (The Minerals, Metals & Materials Society), 2012

INVESTIGATION ON THE PRECIPIPTAION IN MONOCRYSTALLINE AL-MG-SI MODEL ALLOY BY SMALL ANGLE NEUTRON SCATTERING

Cynthia Sin Ting Chang[1], André Heinemann[2], Charles Dewhurst[3], Zeqin Liang[4], John Banhart[1,4]

[1]Technische Universität Berlin; Hardenbergstr. 36/EW 2-3; Berlin, 10623, Germany
[2]Helmholtz-Zentrum Geesthacht; Max-Planck-Straße 1; Geesthacht, 21502, Germany
[3]Institut Laue-Langevin; 6 rue Jules Horowitz; Grenoble Cedex 9, BP 156, F-38042, France
[4]Helmholtz Zentrum Berlin für Materialien und Energie; Hahn-Meitner Platz 1; Berlin, 14109, Germany

Keywords: Al-Mg-Si alloy, Precipitation, SANS, Natural ageing

Abstract

The aim of this work is to clarify the difference in anisotropic precipitate growth in an Al-Mg-Si single crystal during artificial ageing (AA) after different natural pre-ageing (NA) conditions. In one experimental series, in-situ small angle neutron scattering (SANS) experiments were performed at 180°C right after solution heat treatment and quenching. In another series, the crystal was first naturally aged at 'room temperature' for 1 week before AA, after which SANS experiment was carried out. The measurements were performed at D22 of the Institut Laue-Langevin with the single crystal mounted so that the neutron beam was parallel to one of the $\{001\}_{Al}$ directions. Anisotropic scattering from the needle-like precipitates growing along $\{001\}_{Al}$ was observed. The size evolution of the precipitates is compared for the crystal aged with and without NA. For this crystal without NA, the length of the precipitates increases significantly in the first 2h of AA. After this both the length and radius increase with AA time. With NA before AA, the number density of the precipitates is lower comparing to the directly AA crystal. The rate of increase in length of β'' is lower and the mean size of β'' is smaller.

Introduction

Al-Mg-Si alloys are used as car body panels due to their combination of strength and formability. During paint baking of the car – usually 20 min at 180°C – needle-shaped strengthening precipitates β'' are formed in the alloy after prior solutionising and quenching. If the alloy is stored at room temperature after quenching and before AA, the aspect ratio and the number density of the needle-shaped precipitates during AA will be influenced [1]. This is due to the nanoclusters that have formed during storage which, however, are hard to reveal by transmission electron microscopy (TEM) or 3-D atom probe [2]. Although much research has been carried out on this phenomenon [3,4], the influence of clustering on subsequent ageing is not yet fully understood. The size evolution of precipitates in Al-Mg-Si alloys are usually investigated using a conventional microscopic technique e.g. TEM [5]. Sample preparation for such experiment is tedious and normally ex-situ ageing studies are performed to study the size evolution of β''. On the other hand, the volume measured using SANS is around 6 orders of magnitude larger than by TEM, thus providing better statistics for the characterisation of precipitates. In addition, in-situ experiments can be performed so that only one sample is required, allowing us to obtain more reliable information on the size and volume evolution of the precipitates during AA. Such experiments are the basis of this study.

Experimental Setup

A 4.55-cm thick Al-Mg-Si single crystal with surfaces parallel to the (100) plane was produced at the Leibniz Institute for Solid State and Materials Research Dresden. For the first set of SANS measurements the sample was directly measured after solution heat treatment (SHT) at 540°C for 1 h and ice water quenching. In the second set of experiments the crystal was stored at room temperature, i.e. NA for 1 week after SHT and before the SANS experiment.

In-situ experiments at 180°C were performed at instrument D22 at the ILL. The crystal was mounted so that the neutron beam was parallel to one of the $\{001\}_{Al}$ planes. It was also contacted with a hot plate in which the temperature was monitored so that the measuring temperature was maintained at 180°C. In order to avoid moving the sample detector through long distances, the sample was aligned so that only two sample-detector distances, i.e. 1.4 and 5.6 m were used with a neutron wavelength of λ=5 Å to cover a Q-range from 0.015 to 0.41 $Å^{-1}$. Neutron scattering patterns were acquired with a 2-D detector and saved every 5 min, so that with the above configuration, the time resolution of the in-situ experiment is 10 min. After the experiments, the transmission values for the samples were calculated using empty beam data. The background subtraction was performed using Cd. All data reduction and averaging procedures were performed using the $GRAS_{ans}P$ software.

To obtain complementary information the microstructure of the crystal after SHT, quenching and artificial ageing (AA) at 180°C for 8h was characterized by TEM in a Philips EM400 microscope operated with 100 kV. Thin foils suitable for TEM investigations were prepared by electrochemical jet polishing using HNO_3-CH_3OH electrolyte.

Results and Discussion

Figure 1(a) shows the morphology of the precipitates of crystal after 8h of AA obtained by TEM through strain contrast. The electron beam was perpendicular to one of the $\{100\}_{Al}$. The precipitates are expected to be needle-like β'', with $(010)_{\beta''}//(001)_{Al}$ [6]. A corrected 2-D neutron intensity plot of the same condition is shown in Figure 1(b). Anisotropic scattering is observed at α=45°, where α is the angle between Q and the $\boldsymbol{Q}$-vector if the 2-D detector is in the detector plane, indicating scattering from needle-like β''.

Radial averaging of the 2-D neutron intensity data is applied. The resulting 1-D averaged intensities as a function of Q for both the crystal with directly AA and NA before AA are shown in Figure 2(a) and (b), respectively. For short AA from 2 min to around 30 min, the neutron intensity at $Q < 0.1Å^{-1}$ increases indicating that precipitates of around 2 nm have formed. With longer AA a broad hump is observed in the Q range covering $0.03<Q<0.2$ $Å^{-1}$. The amplitude and the width of the hump increase with AA showing that the number and size of the precipitates increase. For the crystal which has been NA for 1 week before AA, see Figure 2(b), neutron scattering is much smaller compared to the sample which has been directly AA. An obvious hump could only be observed after 4 h of AA. Moreover, scattering from the precipitates does not evolve as fast as in the sample directly AA.

Averaged 1-D data provide only a general picture of the changes in scattered neutron intensity with AA. 1-D data is the result of averaging scattering contributions from both the cross-section and the long side of the precipitates. In order to distinguish between the two, 2-D data is selected according to Figure 3(a). The sectors with orange borders enclose the 2-D data representing

scattering from the long side of *β''* precipitates, while the sectors with green borders account for isotropic contributions such as from the cross-section of *β''*. Since contribution from isotropic scattering in *β''* sector cannot avoid, the range of α in each sector is 15° and is chosen so that the overlap of scattering from the isotropic contributions in the *β''* sector is minimized.

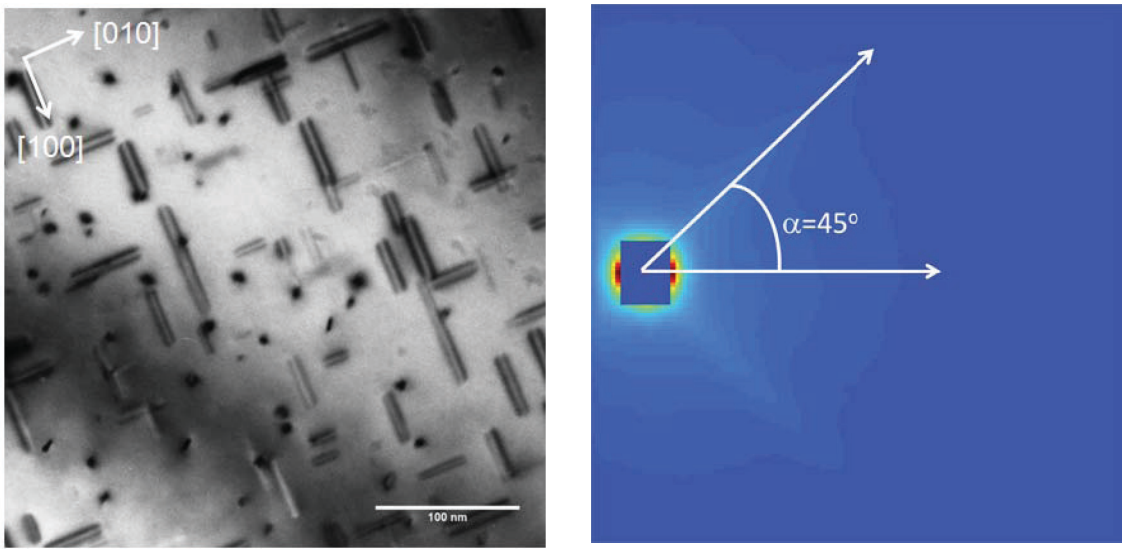

(a) (b)

Figure 1. (a) TEM image of single crystal AA for 8h showing precipitates growing along $<100>_{Al}$ (b) 2-D plot of neutron intensity at a detector distance of 5.6 m scattered from sample in the same condition as in (a). Anisotropic scattering from needle like precipitates at α=45° is seen.

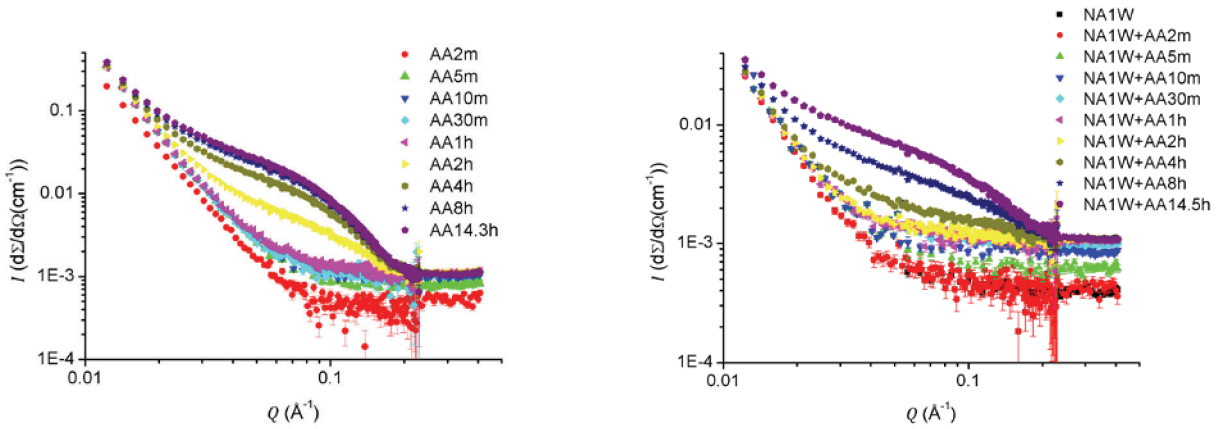

(a) (b)

Figure 2. Scattering cross section vs. Q for crystal, (a) directly AA for different times and, (b) NA for 1 week before AA for different AA times.

Figure 3(b) shows the neutron intensity against Q after radial averaging over the sectors of the crystal directly AA for 14.3 h. Clearly, the scattering from the long side of β'' is stronger than from the cross-section. The intensity curves are fitted by Gaussian functions and a factor $x(Q)$ is obtained,

$$x(Q) = \frac{I_{\beta''}}{I_{isotropic}}\ , \qquad (1)$$

where $I_{\beta''}$ and $I_{\text{isotropic}}$ are the neutron intensities from the long side and the cross-section of β'' respectively. Figure 4(a) and (b) show $x(Q)$ vs. Q. For matters of comparison, the maximum value of $x(Q)$ and the $2\pi/Q$ values of the peak position of the $x(Q)$ curves are given as a function of AA time in Figure 5(a) and (b).

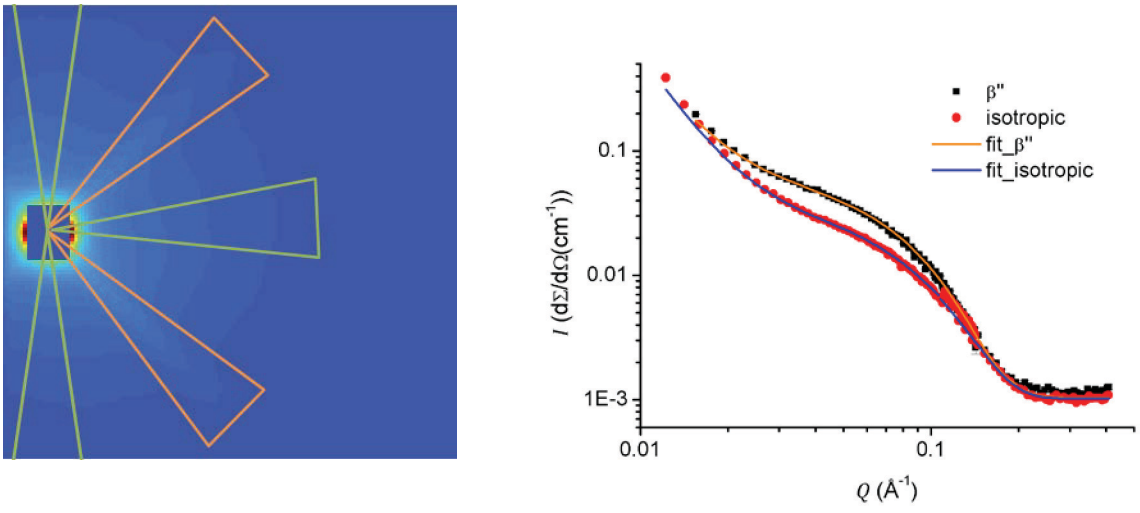

(a) (b)

Figure 3. (a) 2-D plot of neutron intensity at a detector distance of 5.6 m scattered from the crystal after direct AA for 14.3 h. The triangles shown are sectors used for radial averaging; triangles with orange and green borders represent scattering from β'' and isotropic scattering, respectively. (b) Scattering cross section against Q from different sectors as shown in (a).

For the crystal directly AA after quenching, see Figure 4(a), $x(Q)$ increases significantly during the first 2 h of AA and reaches a peak value of ~1.6 which then remains largely the same for further AA, see Figure 5(a), while the position of the peak given by $2\pi/Q$ increases continuously with AA time, see Figure 5(b). If the peak position $2\pi/Q$ of the $x(Q)$ curve is related to the mean size of β'', whereas $x(Q)$ is related to its aspect ratio, the results suggest that the average size of β'' increases significantly within the first 2 h of AA by an increase of length only. After this, both the length and radius of β'' increase and so the average size too. It should be noted that $2\pi/Q$ for 8 h of AA is around 12 nm, which is smaller than what is observed by TEM, see Figure 1(a). This is because $2\pi/Q$ accounts for the average contribution from the length and cross section, Figure 3(b), and this will lead to a smaller value.

For the crystal which has been NA for 1 week before AA, Figure 4(b), an obvious peak in the $x(Q)$ curve cannot be observed before 4 h of AA due to weaker scattering from precipitates, possibly because the number density of β'' is much lower in this crystal than in the one AA without NA, see Figure 2(b). The peak value of $x(Q)$ also increases with AA time and reaches a similar value as in Figure 5(a), but still continues to increase after 14.5 h of AA. The peak position $2\pi/Q$ increases with time up to ~8.5 nm after 14.5 h of AA, see Figure 5(b). The rate of increase of the length of β'' is lower and the mean size is smaller in the sample NA before AA than in the sample AA without NA.

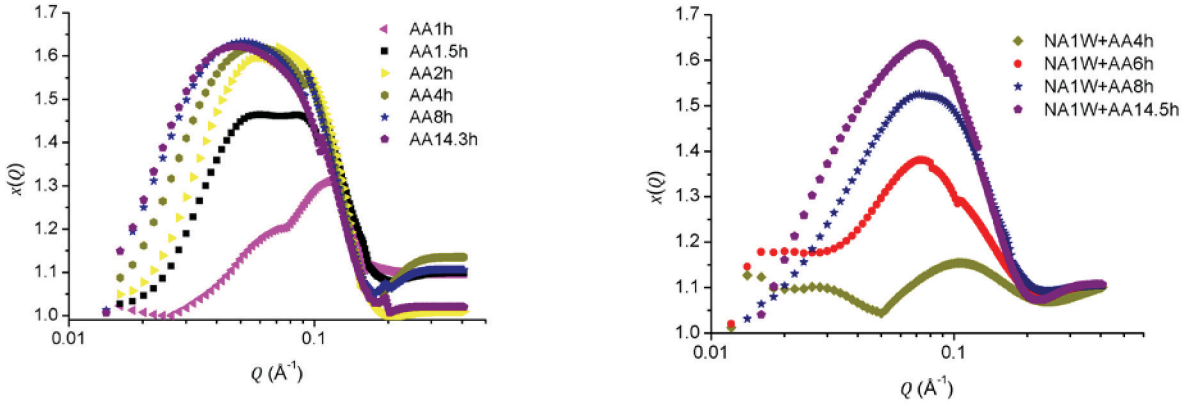

(a) (b)

Figure 4. $x(Q)$ versus Q for the crystal, (a) directly AA and, (b) NA for 1 week before AA, both given for different AA times.

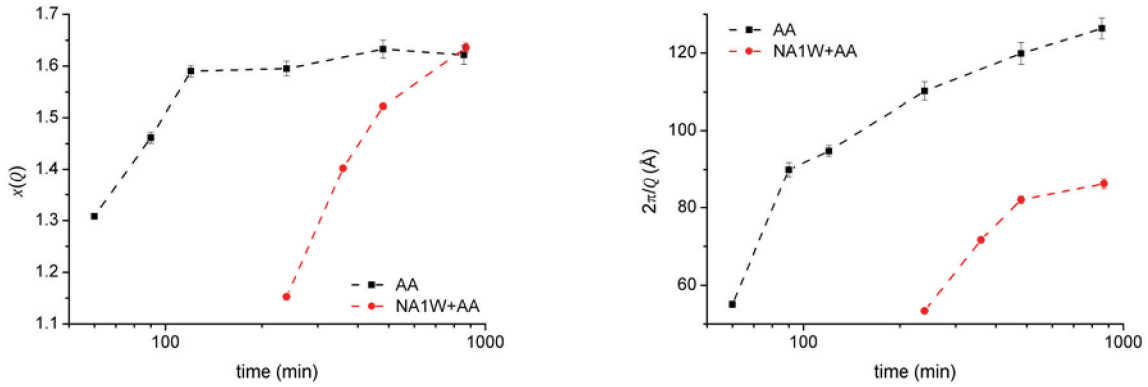

(a) (b)

Figure 5. (a) Maximum values of $x(Q)$ and, (b) $2\pi/Q$ as a function of AA time for the sample directly AA ('AA') and NA for 1 week before AA 'NA1W+AA' .

Conclusions

In-situ SANS measurements at 180°C were performed for an Al-Mg-Si single crystal for two different heat treatments. The following can be observed,

1. The number density of *β''* is much higher when the crystal is directly artificially aged (AA) after quenching than when natural ageing (NA) is carried out before AA.
2. For the directly AA crystal, the length of *β''* increases significantly within the first 2 h of AA and only then both the radius and length increase slightly.
3. Compared to the crystal without NA before AA, the rate of increase in length of *β''* is slower and the mean size is smaller in the sample NA before AA.

Acknowledgements

We would like to thank Dr. Urs Gasser for helping us to perform preliminary SANS experiments in SANS-II at SINQ in the Paul Scherrer Institut.

References

1. J. Banhart, C. S. T. Chang, Z. Liang, N. Wanderka, M. D. H. Lay, A. J. Hill, ,‘‘Natural ageing in Al-Mg-Si alloys- a process of unexpected complexity,’’ *Adavnced Engineering Materials*, 12 (2010) 559.
2. C. S. T. Chang, I. Wieler, N. Wanderka, J. Banhart, “Positive effect of natural pre-ageing on precipitation hardening in Al-0.44at%Mg-0.38at%Si alloy,” *Ultramicroscopy*, 109 (2009) 585.
3. C. S. T. Chang, J. Banhart, “Low-temperature differential scanning calorimetry of an Al-Mg-Si alloy,” *Metallurgical and Materials Transactions* A, 42 (2011) 1960.
4 . J. Banhart, M. D. H. Lay, C. S. T. Chang, A. J. Hill, “The kinetics of natural ageing in Al-Mg-Si alloys studied by positron annihilation spectroscopy,” *Physical Review B*, 83 (2011) 014101.
5. C. D. Marioara, S. J. Anderson, H. W. Zandbergen, R. Holmestad, “The influence of alloy composition on precipitates of the Al-Mg-Si system,” *Metallurgical and Materials Transactions* A, 36 (2011) 691.
6. S. J. Anderson, H. W. Zandbergen, J. Jansen, C. Træholt, U. Tundal and O. Reiso, “The Crystal Structure of the β‘‘ Phase in Al-Mg-Si Alloys,” *Acta Materialia*, 46 (1998), 3283.